Zinc controls PML nuclear body formation through regulation of a paralog specific auto-inhibition in SUMO1

*Mathieu Lussier-Price[1], Haytham M. Wahba[1,2], Xavier H. Mascle[1], Laurent Cappadocia[1, 4], Veronique Bourdeau[1], Christina Gagnon[1], Sebastian Igelmann[1], Kazuyasu Sakaguchi[3], Gerardo Ferbeyre[1] and James G. Omichinski[1] **

[1] Département de Biochimie et Médicine Moléculaire, Université de Montréal, Montréal, QC Canada, [2]Department of Biochemistry, Beni-Suef University, Beni-Suef, Egypt and [3]Department of Chemistry, Faculty of Science, Hokkaido University, Sapporo, Japan.

[4] Current Address : Département de Chimie, Université de Québec à Montréal, Montréal, QC, Canada

***Correspondence**:

James G. Omichinski, Département de Biochimie et Médicine Moléculaire, Université de Montréal C.P. 6128 Succursale Centre-Ville, Montréal, QC H3C 3J7 Canada. Email:

jg.omichinski@umontreal.ca

Running Title: *Zinc enhances PML nuclear body formation*

TABLE S1 Thermodynamic parameters for the effect of SUMO and ΔN-SUMO proteins with peptides from the SIM regions of PML and Daxx as well as UBC9UBC9

Protein in Cell [a]	**Protein in Syringe** [a]	**K_D (μm)**	**ΔH (kcal/mol)**	**-TΔS (kcal/mol)**	**ΔG_{ITC}** [b] **(kcal/mol)**
SUMO1	PML-SIM	44 ± 5	0.50 ± 0.04	-6.45 ± 0.10	-5.93 ± 0.05
ΔN-SUMO1	PML-SIM	58 ± 2	2.12 ± 0.22	-7.90 ± 0.21	-5.75 ± 0.05
SUMO1	PML-SIM-4SD	11 ± 2	5.25 ± 0.03	-12.0 ± 0.1	-6.76 ± 0.08
ΔN-SUMO1	PML-SIM-4SD	0.52 ± 0.02	6.51 ± 0.05	-15.1± 0.1	-8.58 ± 0.02
SUMO1	Daxx-SIM-2SD	2.8 ± 0.6	5.10 ± 0.54	-12.7± 0.6	-7.60 ± 0.12
ΔN-SUMO1	Daxx-SIM-2SD	0.34 ± 0.05	4.52 ± 0.03	-13.4 ± 0.1	-8.84± 0.08
SUMO1	Daxx-SIM-PO4	0.88 ± 0.12	1.62 ± 0.52	-9.89 ± 0.43	-8.30 ± 0.06
ΔN-SUMO1	Daxx-SIM-PO4	0.10 ± 0.02	1.61 ± 0.35	-11.2 ± 0.5	-9.52 ± 0.10
SUMO1	UBC9	0.029 ± 0.011	-2.67 ± 0.53	-7.67 ± 0.75	-10.3 ± 0.2
ΔN-SUMO1	UBC9	0.073 ± 0.015	-3.24 ± 0.35	-6.52 ± 0.23	-9.75 ± 0.12
SUMO2	PML-SIM-4SD	5.3 ± 1.0	1.14 ± 0.14	-8.34 ± 0.02	-8.34 ± 0.02
ΔN-SUMO2	PML-SIM-4SD	2.9 ±0.7	2.18 ± 0.40	-9.77 ± 0.22	-9.77 ± 0.22
SUMO2	Daxx-SIM-2SD	1.0 ± 0.1	2.12 ± 0.23	-10.3 ± 0.2	-8.16 ± 0.06
ΔN-SUMO2	Daxx-SIM-2SD	0.51 ± 0.11	1.48 ± 0.09	-10.1 ± 0.1	-8.60 ± 0.13
N2-SUMO1	PML-SIM-4SD	1.4 ± 0.1	6.72 ± 0.91	-14.7 ± 0.9	-7.95 ± 0.02

[a] All experiments were conducted in 25 mM Tris buffer pH7.4

b $\Delta G_{ITC} = -RT\ln(K_A)$ at $T = 298.15$ K.

TABLE S2 Thermodynamic parameters for the effect of metals on PML-SIM interactions with SUMO1, SUMO2 and the SUMO1E11Q variant proteins.

Protein in Cell [a]	**Protein in Syringe** [a]	**Metal**	**K_D (μm)**	**ΔH (kcal/mol)**	**-TΔS (kcal/mol)**	**ΔG_{ITC}** [b] **(kcal/mol)**
SUMO1	PML-SIM	-	155 ± 2	0.76 ± 0.06	-5.96 ± 0.06	-5.20 ± 0.01
SUMO1	PML-SIM	Zn	42 ± 8	1.79 ± 0.61	-7.75 ± 0.48	-5.98 ± 0.11
SUMO1	PML-SIM-4SD	-	22 ± 1	5.27 ± 0.20	-11.6 ± 0.1	-6.36 ± 0.01
SUMO1	PML-SIM-4SD	Zn	0.57 ± 0.08	2.81 ± 0.34	-11.3 ± 0.3	-8.52 ± 0.09
SUMO1	PML-SIM-4SD	Ca	22 ± 3	3.17 ± 0.01	-9.54 ± 0.06	-6.35 ± 0.06
SUMO2	PML-SIM-4SD	-	12 ± 1	0.56 ± 0.31	-7.29 ± 0.28	-6.73 ± 0.01
SUMO2	PML-SIM-4SD	Zn	6.5 ± 1.2	2.50 ± 0.31	-9.59 ± 0.41	-7.09 ± 0.11
SUMO1E11Q	PML-SIM-4SD	-	8.7 ± 1.4	3.25 ± 0.97	-10.2 ± 0.9	-6.91 ± 0.09
SUMO1E11Q	PML-SIM-4SD	Zn	4.2 ±1.3	6.68 ± 2.03	-14.0 ± 2.9	-7.33 ± 0.16

[a] All experiments were conducted in 25 mM Tris buffer pH7.4 with 50 mM NaCl in the presence of absence of 1 mM of metal ($ZnSO_4$ or $CaCl_2$)

[b] $\Delta G_{ITC} = -RT\ln(K_A)$ at $T = 298.15$ K.

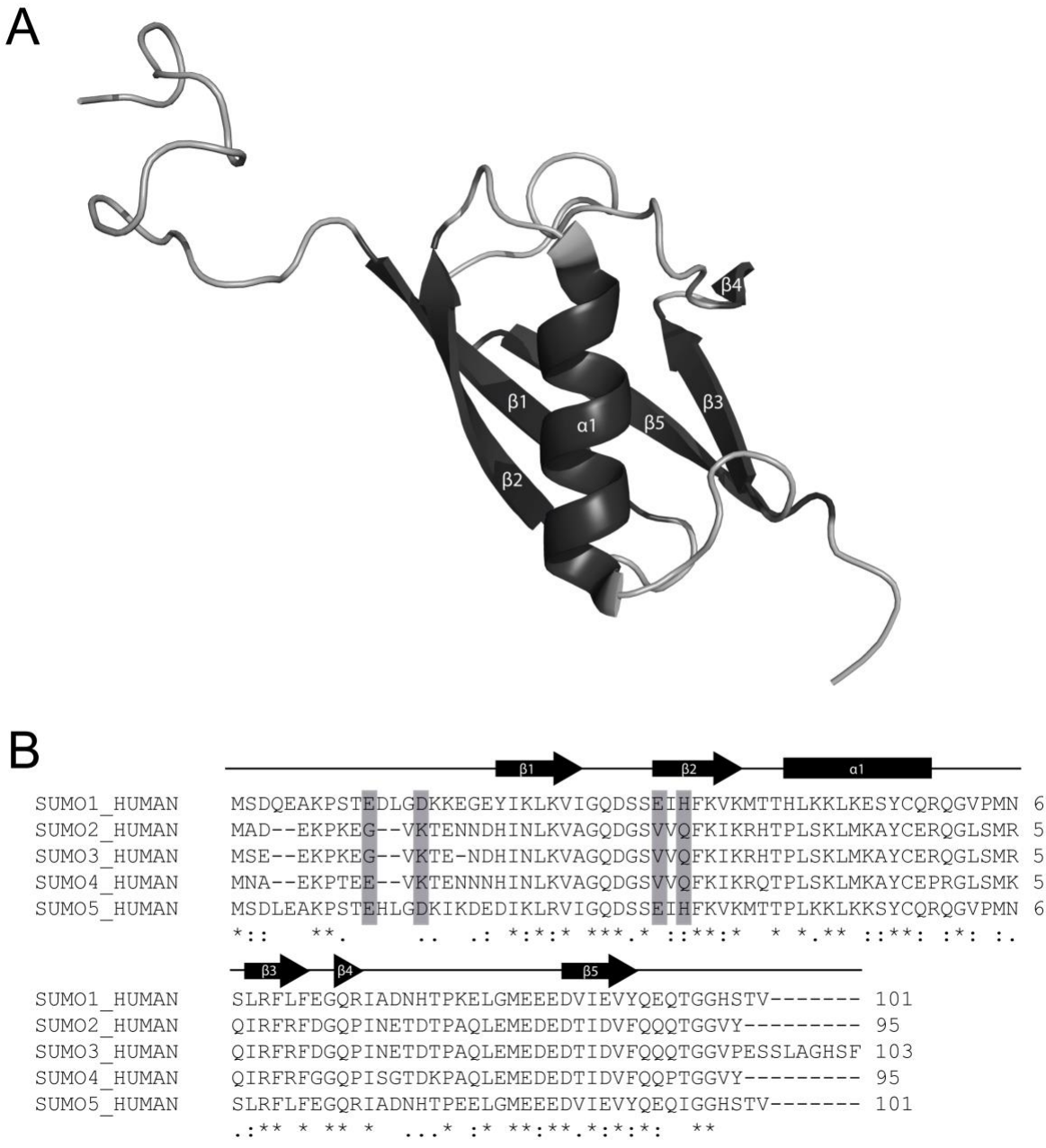

Supplemental Figure S1. Sequence alignment of the five identified human SUMO1 proteins. (**A**) Cartoon representation of the NMR structure of full length SUMO1 (PDB:2NV1) highlighting its secondary structure elements (dark gray). (**B**) Sequence alignment of the five human SUMO paralogs. The secondary structure elements are highlighted above the sequence with either arrows (strands) or a square (helix). The residues involved in binding to zinc in the crystal structure of the complex of SUMO1:PML-SIM-4SD:Zn are shaded in grey.

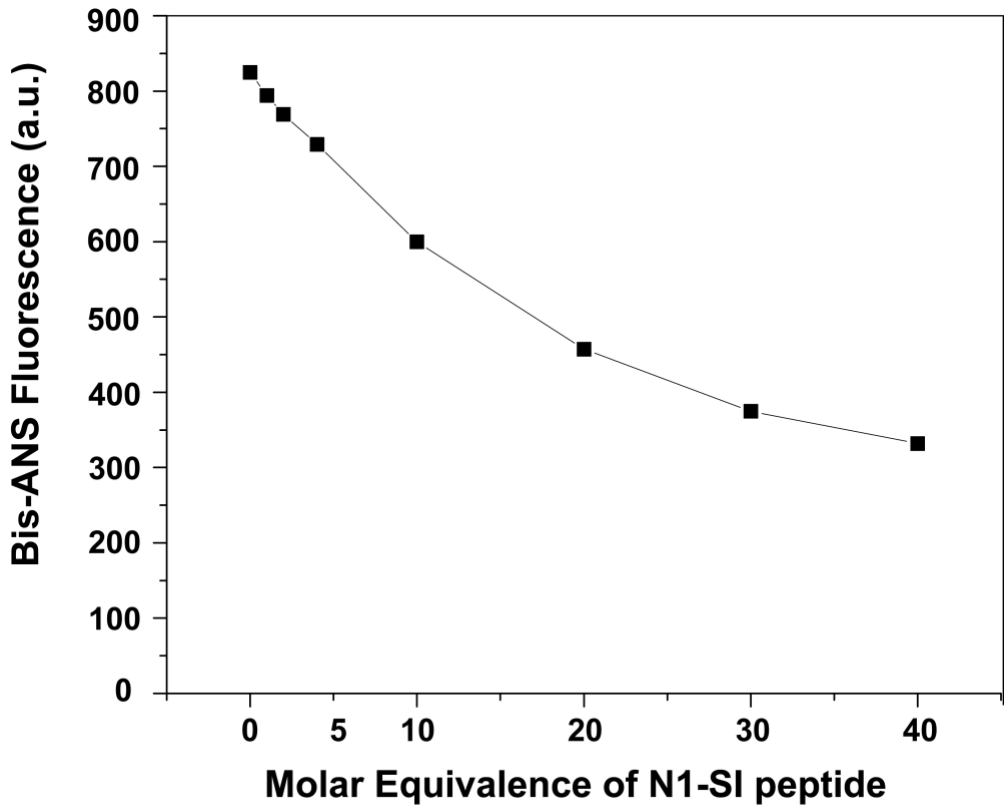

Figure S2. The N-terminal of SUMO1 inhibits interactions with the SIM-binding interface. Graphical plot of the bis-ANS fluorescence signal recorded at 487 nm in the presence of ΔN-SUMO1 following addition of various amounts (0 to 40 molar equivalence) of the N1-S1 peptide.

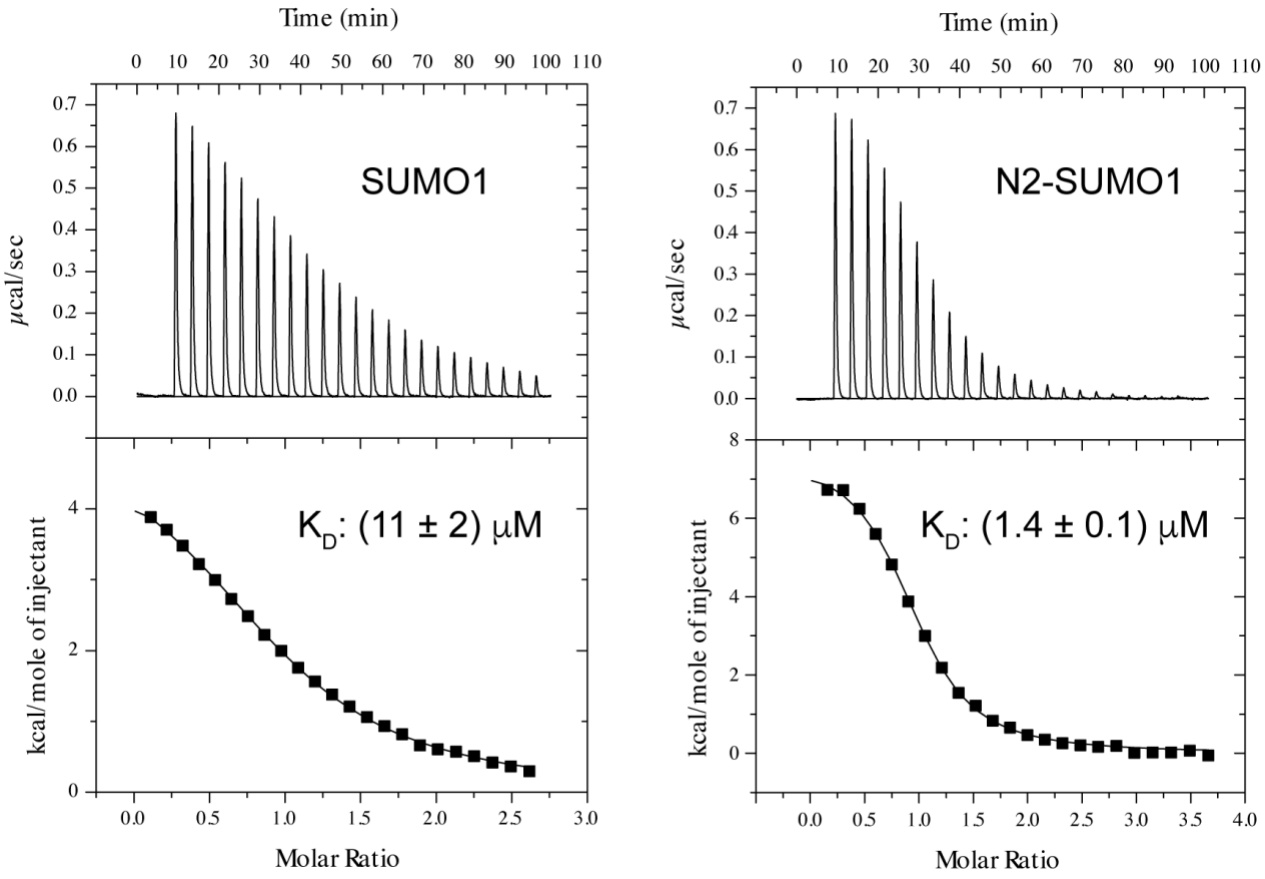

Supplemental Figure S3. The N-terminal of SUMO2 does not inhibit binding of phosphorylated SIMs. ITC thermograms for the titration of PML-SIM-4SD with either SUMO1 (**left panel**) or the N2-SUMO1 (**right panel**) chimeric protein. The K_D values (in μM) obtained in ITC studies are included on the respective thermogram.

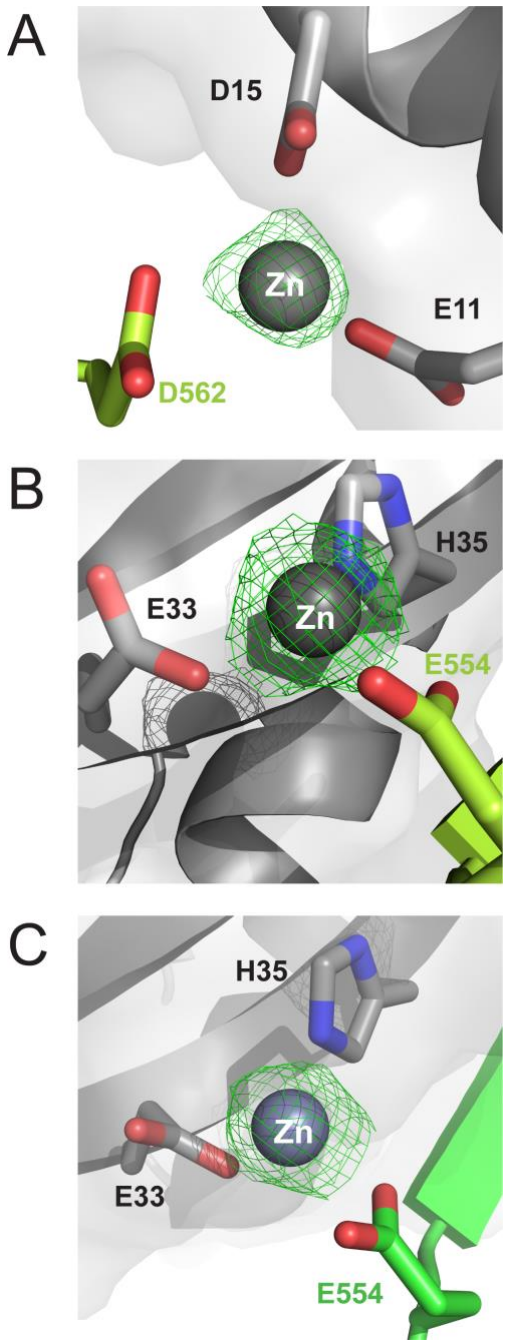

Supplemental Figure S4. Structural characterization of a SUMO1:PML-SIM:Zn and SUMO1:PML-SIM:Zn complexes. Simulated annealing maps highlighting the zinc-binding sites in complexes of SUMO1 with PML-SIM-4SD and PML-SIM. The occupancies of Zn ions in the complexes were set to zero prior to calculating the simulated annealing omit maps using Phenix. (**A**) Close-up of Zn1 bound between SUMO1 and PML-SIM-4SD. (**B**) Close-up of Zn2 bound between SUMO1 and PML-SIM-4SD. (**C**) Close-up of Zn bound between SUMO1 and PML-SIM. The residues involved in binding the zinc atoms are in stick representation and a 1.5σ cut-off was used to generate the F_oF_c maps.

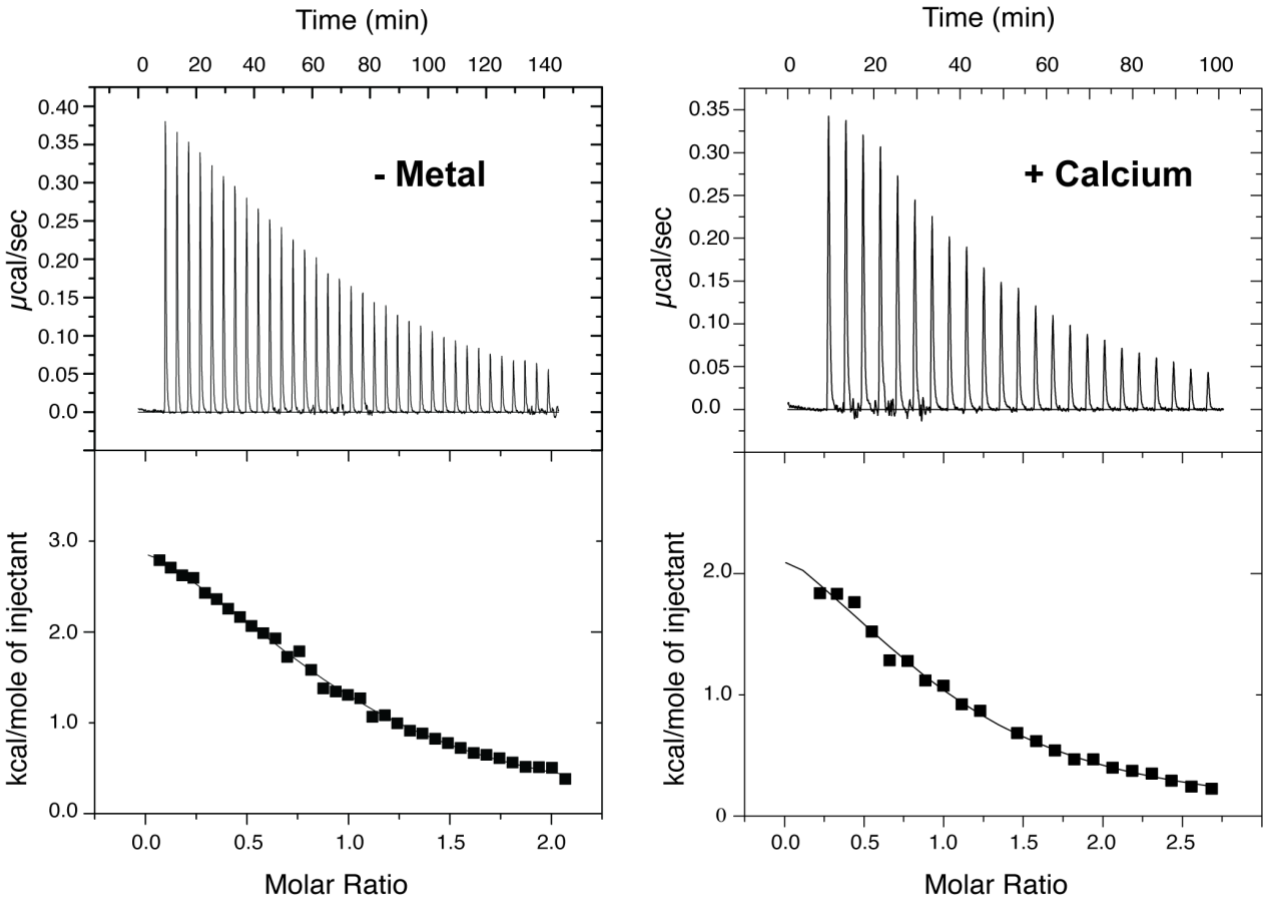

Supplemental Figure S5. Zinc ions specifically enhance binding of the phospho-mimetic SIM of PML to SUMO1.Comparison of the ITC thermogram from the titration of PML-SIM-4SD with SUMO1 in the absence (**left panel**) or the presence calcium chloride (**right panel**). Experiments were conducted in 20 mM Tris-HCl pH7.4 , 50 mM NaCl in the absence or presence of 1 mM $CaCl_2$.

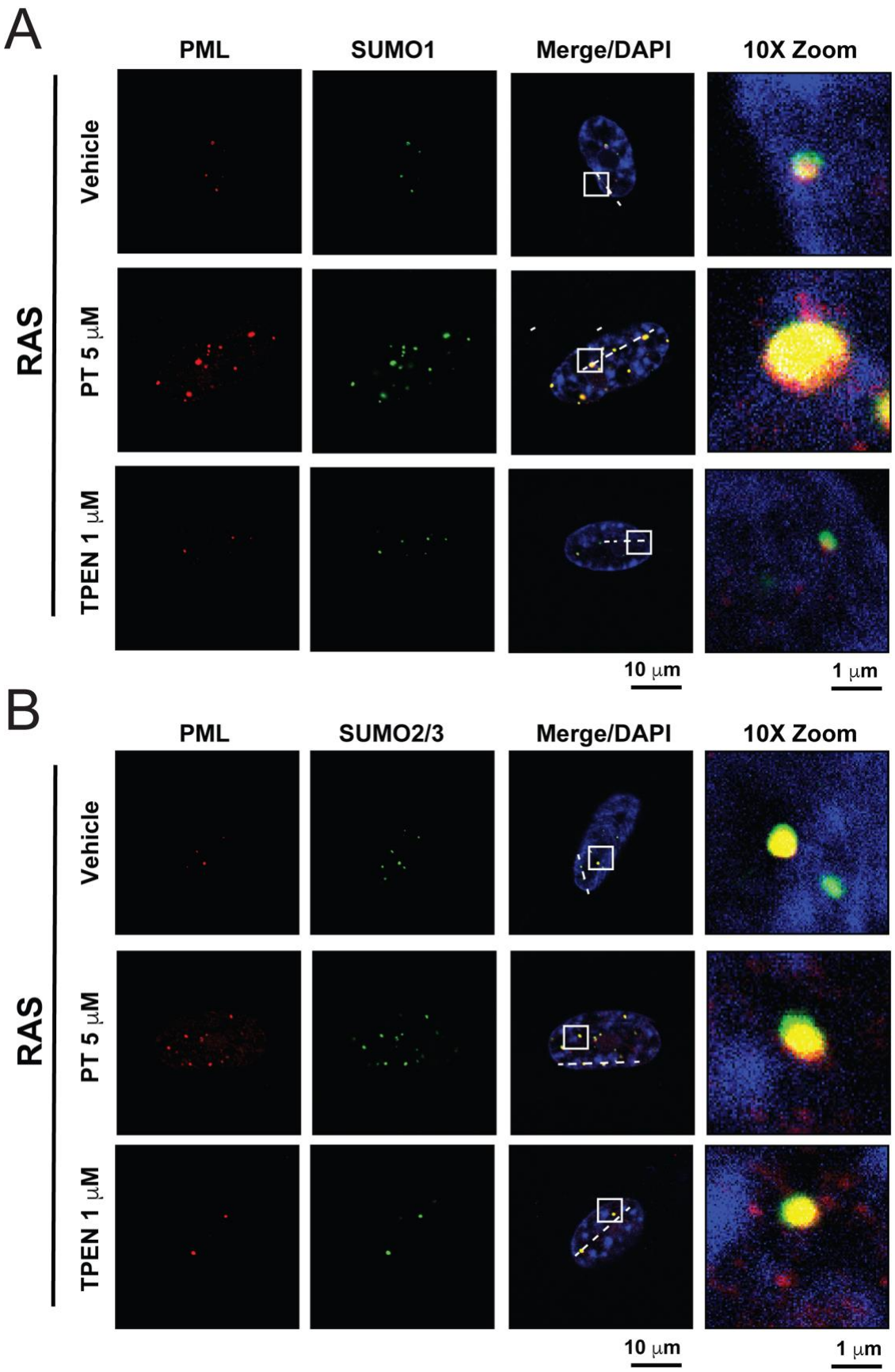
A
PML
SUMO1
Merge/DAPI
10X Zoom
RAS
Vehicle
PT 5 μM
TPEN 1 μM
10 μm
1 μm
B
PML
SUMO2/3
Merge/DAPI
10X Zoom
RAS
Vehicle
PT 5 μM
TPEN 1 μM
10 μm
1 μm

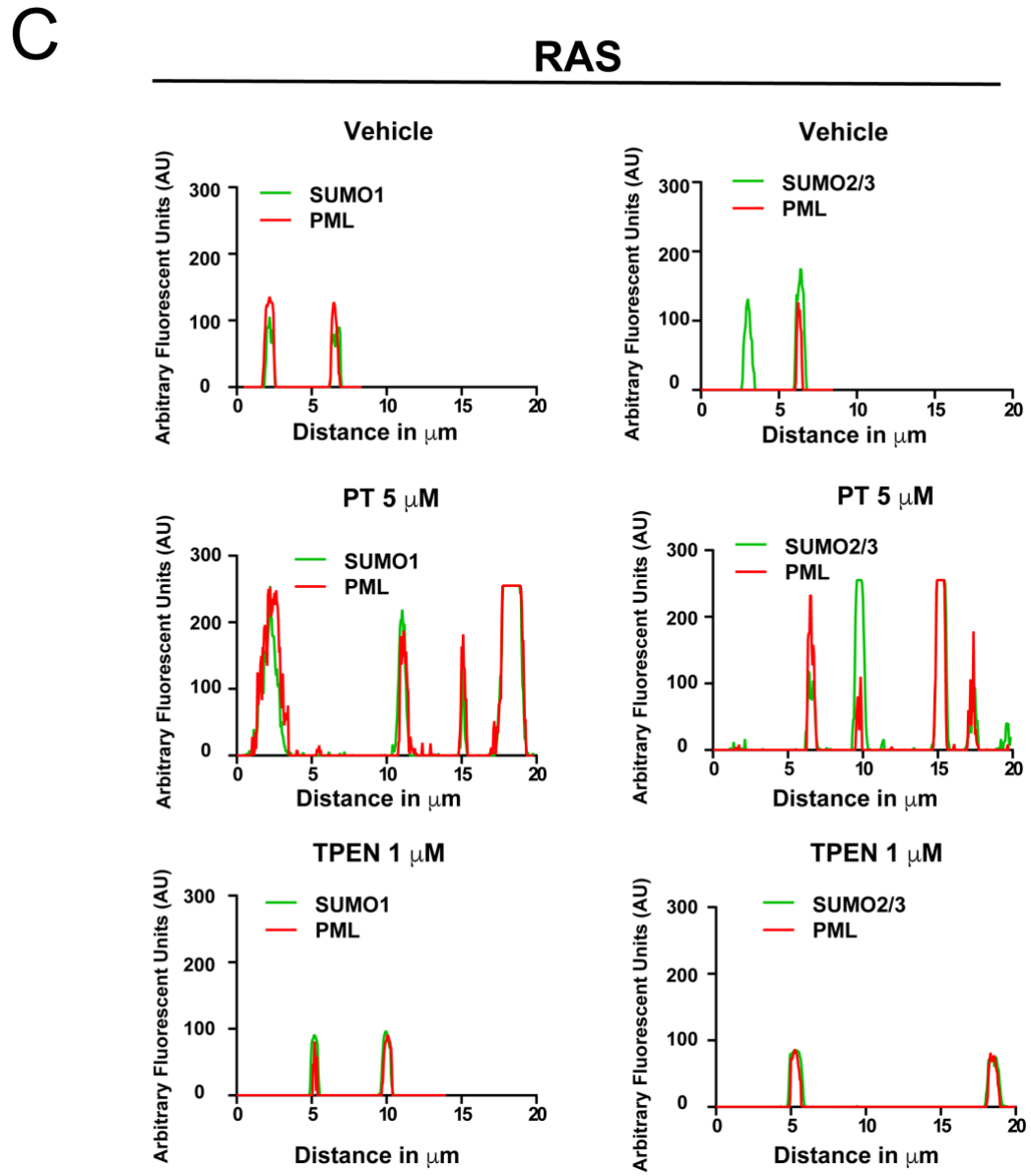

Supplemental Figure S6. Increasing cellular zinc levels in senescent cells enhances SUMO1 and SUMO2/3 levels in PML-NBs. Normal human fibroblasts IMR90 cells expressing the activated RAS oncogene, to induce senescence were treated for 24h with either control vehicle, 5μM PT (pyrithione) or 1μM tetrakis(2-pyridinylmethyl)-1,2-ethanediamine (TPEN) prior to fixation and indirect immunofluorescence with a specific anti-PML primary antibody and either a specific anti-SUMO1 (**A**) or anti-SUMO2/3 (**B**) primary antibody and corresponding secondary fluorescent antibody as well as with DAPI to stain DNA in the nucleus. Zoomed regions are indicated by white squares(**C**) The relative fluorescence intensity of either SUMO1 and PML or SUMO2-3 and PML were determined with Image J using the linear histogram intensity plugin as previously shown (50). Briefly, a line was drawn through the image containing several PML/SUMO foci, and then the intensity of fluorescent was extracted. Dotted lines in (**A**) and **(B**) for the three treatments group (Vehicle, PT and TPEN) indicate the areas which were extracted for the intensity measurements.

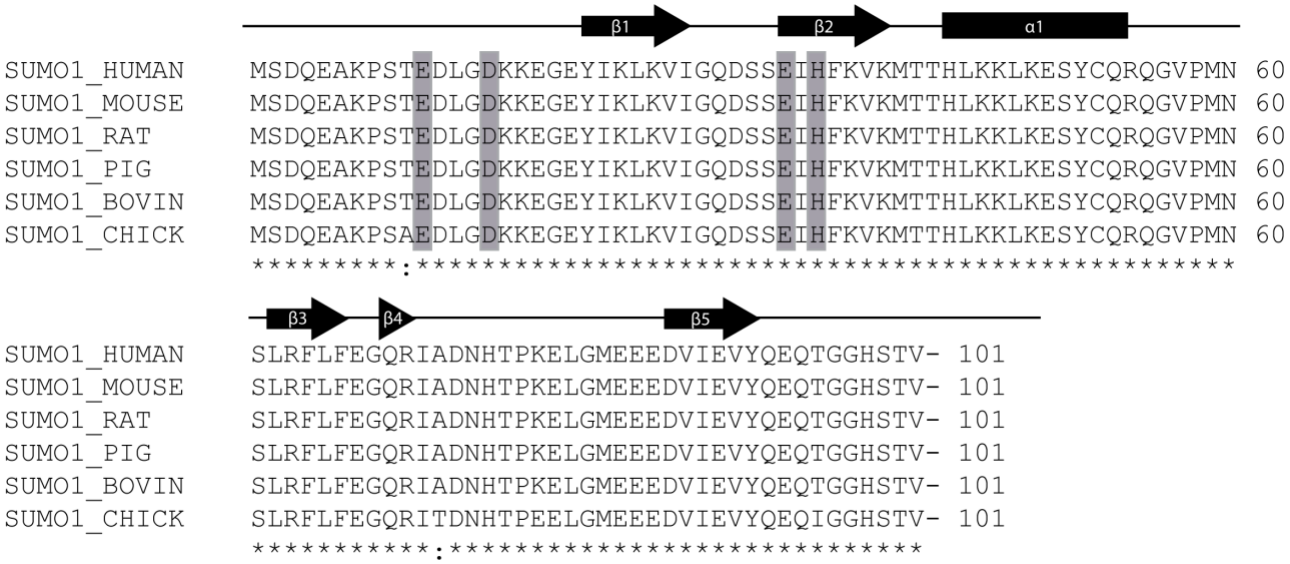

Supplemental Figure S7. Sequence alignment of SUMO1 from several different mammals. The secondary structure elements are highlighted above the sequence with either arrows (strands) or a square (helix). The residues involved in binding to zinc in the crystal structure of the complex of SUMO1:PML-SIM-4SD:Zn are shaded in grey.